

Photoluminescence clamping with few excitons in a single-walled carbon nanotube

Y.-F. Xiao, T.Q. Nhan, M.W.B. Wilson, and James M. Fraser

*Department of Physics, Engineering Physics & Astronomy,
Queen's University, Kingston, Ontario, K7L 3N6 Canada*

(Dated: May 27, 2022)

Single air-suspended carbon nanotubes (length 2 - 5 μm) exhibit high optical quantum efficiency (7 - 20%) for resonant pumping at low intensities. Under ultrafast excitation, the photoluminescence dramatically saturates for very low injected exciton numbers (2 to 6 excitons per pulse per SWCNT). This PL clamping is attributed to highly efficient exciton-exciton annihilation over micron length scales. Stochastic modeling of exciton dynamics and femtosecond excitation correlation spectroscopy allow determination of nanotube absorption (2 - 6%) and exciton lifetime (85 ± 20 ps).

PACS numbers: 78.67.Ch, 71.35.-y, 78.55.-m, 78.47.jc, 42.64.Re

Understanding the electronic and optical properties of single-walled carbon nanotubes (SWCNTs) will no doubt benefit the development of carbon-based optoelectronic devices [1, 2, 3]. Great advances have been made in synthesizing SWCNTs of higher quality and isolating them from perturbations [4, 5, 6] with a general trend from measurement on ensemble towards single tube level [7, 8, 9, 10]. For encapsulated SWCNTs, exciton many-body interactions manifest themselves in sublinear photoluminescence emission (PL) and is well explained by diffusion limited exciton-exciton annihilation [11, 12], with diffusion lengths of 6 - 90 nm [10, 13]. The recent observation of photon antibunching in SWCNT PL is also consistent with exciton localization or very efficient exciton-exciton annihilation [9]. It has been shown that processing affects linear properties [14], but the effect that sonification and encapsulation might have on exciton interactions is not well understood.

By studying a single air-suspended, unprocessed SWCNT [7, 15], we hope to reduce ambiguities posed by environmental effects and isolate the inherent SWCNT properties and exciton dynamics. In this letter, we report on studies of PL fluence (emission from E_{11} van Hove singularity excitons) as a function of pump fluence (resonant to E_{22} excitons) on single (9,8) and (10,8) SWCNTs, using optical 150 fs pulse, 4 ps pulse, and continuous-wave (CW) excitation. Unperturbed SWCNTs are studied by selecting relatively bright SWCNT that exhibit narrow room temperature emission (~ 12 meV) and absorption (~ 44 meV) linewidths. They are also sufficiently long that we can resolve their lengths using high resolution PL mapping. Under low excitation, PL output relative to incident fluence shows a linear dependence and a large PL action cross section (defined in Ref. [16]) consistent with high quality SWCNTs. Also similar to encapsulated SWCNTs, exciton linear decay lifetimes are 85 ± 20 ps. In sharp contrast to encapsulated SWCNT behavior, the PL from an air-suspended SWCNT saturates at moderate pump fluence (100 photon/pulse/SWCNT) and does not increase for over an order of magnitude pump increase. Comparison to a stochastic model of exciton decay shows PL clamping is consistent with efficient exciton-exciton annihilation over micron-length scales.

This is considerably longer than expected based on models developed for SWCNTs (exciton diffusion lengths 6 - 90 nm [10, 13]), suggesting that exciton interactions are inherently different in an air-suspended SWCNT.

Air-suspended SWCNTs are grown by chemical vapor deposition on lithographically patterned silicon dioxide on silicon wafers (similar to Ref. [17]). The SWCNTs are suspended on 0.5 μm high ridges. During experimentation, the SWCNT environment is purged with dry N_2 to avoid sample degradation. PL spatial mapping is used to locate bright (9,8) and (10,8) SWCNTs and indicates low SWCNT density (~ 3 bright SWCNTs per mm^2). Photoluminescence excitation spectroscopy and high resolution PL mapping are performed on candidate SWCNT to determine species, quality, length and orientation. SWCNTs analyzed in this letter maintained their PL emission as well as spectral shape throughout the entire investigation.

Results from a typical (9,8) SWCNT (length 4.5 μm) are shown in Figure 1 (a). Optical excitation is by 150 fs duration pulses (Ti:sapphire oscillator at 800 nm center wavelength, 76 MHz repetition rate, linear polarized parallel to SWCNT axis). The SWCNT is quasi-homogeneously excited by setting the excitation beam FWHM (13 μm) larger than the tube length. Total number of photons incident, PI , is determined from the product of pump intensity and surface area of the unrolled tube. Multiple scans for alternatively increasing and decreasing pump fluence show no hysteresis or aging. Photons emitted, PE , is the total photon number emitted per pulse per SWCNT [18]. PL in the region around saturation onset is shown in Figure 1 (b) on a linear scale. At low pump fluence, the slope of PE relative to PI matches CW excitation and its value is the PL action cross section (0.004) which is within a factor of three (higher) compared to previous high quality encapsulated samples [16]. With higher pump fluence, the PL deviates from linear and reaches an onset point ($PI \sim 100$ or 7×10^{11} photon/ cm^2 /pulse) where PE is fully saturated. Most past work on nanotube ensembles reported onset of sublinear behavior at much higher pump fluences (2 - 3 orders of magnitude) and did not observe PL clamping [8, 12, 19]. Nonlinear behavior was attributed

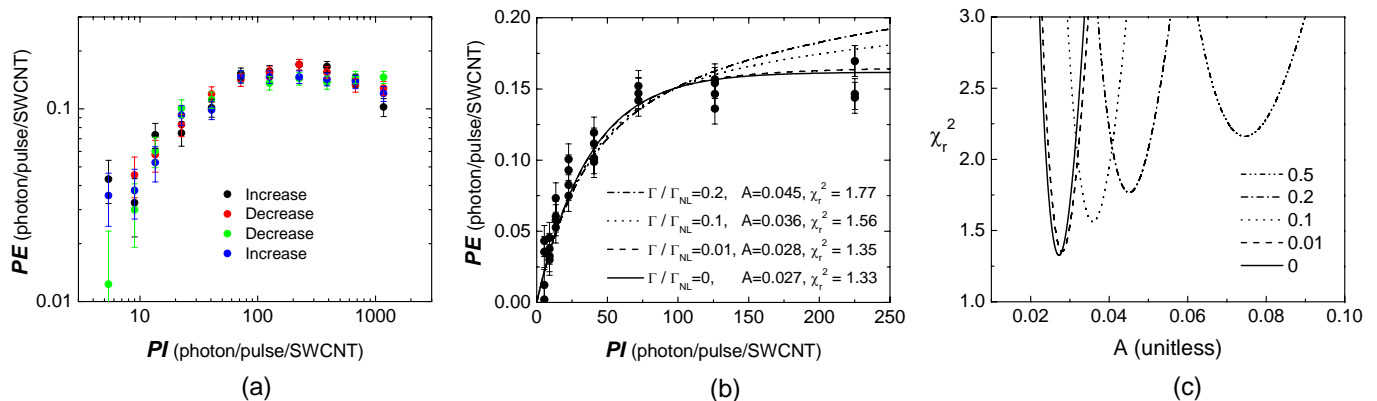


FIG. 1: (a) Single (9,8) SWCNT PL as a function of incident pump fluence (recorded using both increasing and decreasing pump fluences). (b) Experimental data (dots) are compared to results from a stochastic model (solid lines) with various $\frac{\Gamma}{\Gamma_{NL}}$ ratios and absorption coefficients (A). (c) Reduced chi-square as a function of A are calculated at different ratios of $\frac{\Gamma}{\Gamma_{NL}}$.

to exciton-exciton interactions resulting in nonradiative annihilation. A similar hard saturation behavior was recently reported for SDBS-encapsulated SWCNTs measured in confocal configuration by Högele *et al.* [9] at much higher pump fluence (10^{14} photon/cm²/pulse) but they employed a pump resonant to a phonon sideband. In our studies, we have noted that the strong PL clamping is lost when we employ inhomogeneous excitation (smaller pump spot than tube length) [20]. A similar problem would occur for ensemble studies unless the field of view was restricted to the region of the sample that is quasi-uniformly excited (*e.g.* as provided by confocal light collection). An additional problem for random orientated ensemble systems is that the light field couples with variable efficiency depending on SWCNT orientation thus lessening saturation effects for similar intensities. Even so, inhomogeneous excitation or coupling is not expected to account for the dramatic differences in nonlinear PL behavior between air-suspended and encapsulated SWCNTs. A careful examination of the air-suspended SWCNT behavior is required to ascertain if the microscopic processes affecting exciton dynamics are fundamentally different compared to encapsulated samples.

A first question is if air-suspended SWCNTs demonstrate different linear behavior for absorption or emission. PL action cross section is a useful metric since measurement of absorption independently of emission efficiency is not straightforward [16]. By attributing the observed saturation to exciton-exciton annihilation, we can separate the relative contributions to PL action cross section ($A \times \alpha \eta_{QE}$) of absorption (unitless A) and emission (experimentally resolved $\alpha \eta_{QE}$). A is the product of the atomic absorption cross section and carbon surface density [15]. η_{QE} is the intrinsic optical quantum efficiency and $\alpha \leq 1$ due to nanotube imperfections. The results from a detailed stochastic model are described below but it is instructive to determine an upper limit for absorption by assuming annihilation is instantaneous over the

entire SWCNT length. Thus one or more excitons relaxes quickly to just one exciton, which then decays through linear recombination including radiative emission. Under this simple model, since the injection of one or more excitons produces identical PL, the full time dynamics do not need to be modeled to find PL power dependence; all that is relevant is the probability of injecting zero excitons per pump pulse [20]. For ultrafast pulse excitation, the probability of n initial injected excitons (ρ_n) is well modeled by a Poissonian distribution ($\rho_n = \frac{\bar{n}_0^n}{n!} e^{-\bar{n}_0}$, with mean $\bar{n}_0 = A \times PI$ (/pulse/tube)). With instantaneous nonlinear relaxation, the PL scales with $1 - \rho_0 = 1 - e^{-A \times PI}$. When the chance of injecting zero excitons is negligible, the PL is clamped. A fit of this function to the data in Fig 1 (solid curve on 1 (b)) yields an absorption coefficient of $A = 0.027$ which compares with the high end of the range of 0.003 - 0.06 reported by different groups [6, 14, 16, 21, 22, 23, 24]. If one compares this result only with groups who observe similar narrow absorption linewidths, this simple model result is within a factor of two of their estimates [16]. Interestingly enough, this absorption coefficient ($A = 2.7\%$ of photons incident on the SWCNT are absorbed) is quite similar to the measured value for graphene: 2.3% per layer [25].

Though the above model fits the data and provides an upper bound for absorption, it is not clear if the approximation used (instantaneous exciton-exciton annihilation over micron-length scales) is appropriate. By adapting the stochastic model of exciton relaxation, as proposed by Barzykin and Tachiya [26] we examine this in more detail. In contrast to the past work that employed an initial Poissonian distribution over different SWCNTs in an ensemble system, we model the initial Poissonian distribution over many pulses on a single SWCNT. Injection and relaxation from E_{22} to E_{11} are assumed very fast [19, 27] so that initial exciton number at E_{11} is identical to the total photon number absorbed at E_{22} . By numerically solving the coupled rate equations, the average number of excitons per pulse per nanotube as a function of time,

$\bar{n}(\Gamma t)$, can be calculated, where Γ is the linear exciton relaxation rate. The simulation results are compared to the experimental data as following:

$$PI = \frac{\bar{n}(0)}{A} \quad (1)$$

$$PE = \left\{ \int_0^\infty \bar{n}(\Gamma t) d(\Gamma t) \right\} \times \alpha \eta_{QE} \quad (2)$$

Note that the time variable is normalized to Γ . As a result, PE as a function of PI depends only on the relative rates of linear to nonlinear exciton relaxation ($\frac{\Gamma}{\Gamma_{NL}}$). Comparison between theory and experiment is achieved by scaling the slope of the numerical results in the linear regime to match the experimentally determined PL action cross section ($A \times \alpha \eta_{QE}$); thus the number of free parameters is reduced to two. The best fit of simulation to experimental is determined by reduced chi-square minimization (χ_r^2) as a function of $\frac{\Gamma}{\Gamma_{NL}}$ and A (Figure 1 (c)). As illustrated in Figure 1 (b), for four simulated curves at $\frac{\Gamma}{\Gamma_{NL}} = 0, 0.01, 0.1, 0.2$ that have been optimized in terms of A , $\frac{\Gamma}{\Gamma_{NL}} = 0$ and $A = 0.027$ yield the best fit. Note that some SWCNT exhibit a declining trend at higher pump fluence ($PI > 250$) suggesting the presence of a higher order nonlinear process (which is not included in the modeling), thus we fit to below $PI = 250$. To verify this model and resulting values for absorption and decay rate ratio, we compare the PL pump power dependence with 150 fs pulse, 4 ps pulse, and CW excitation. Experimentally, PL from all three scenarios overlap in the linear regime as expected. PL from 4 ps excitation is identical (within experimental uncertainty) to 150 fs excitation, indicating nonlinear excitation and phase-space filling in E_{22} is not playing a role in the saturation process. Modeling exciton dynamics with 4 ps injection requires extending the stochastic model to explicitly include a generation term (*i.e.* we no longer assume an initial Poissonian distribution). For the fit parameters obtained above and a linear relaxation rate of $(90 \text{ ps})^{-1}$ (verified later), calculated PL output for 4 ps is very similar to 150 fs excitation. Increased PL for the same average light intensity is predicted for longer optical pulses (durations on the order of exciton linear lifetime); this is observed with CW excitation which exhibits little saturation over the intensity regime explored.

Similar PL clamping is observed for a variety of both (9,8) and (10,8) SWCNTs (Figure 2). There is some variation of PL action cross sections and maximum PL levels, which does not correlate to length variations and is attributed to tube imperfections still present even in these air-suspended SWCNTs (*i.e.* different α). Fitting the stochastic model to the PL output from each SWCNT provides a range of PL action cross sections: 0.002 - 0.01, absorption coefficients: 0.02 - 0.06, and optical quantum efficiency: 7% - 20% (higher than the 1% - 8% reported by previous work [14, 15, 16, 22]). Though the experimental uncertainty in PL action cross section is approximately 30% and the extraction of quantum efficiency

relies on modeling, the high values determined here are consistent with our expectation that defects and environment effects have been reduced in the air-suspended SWCNT.

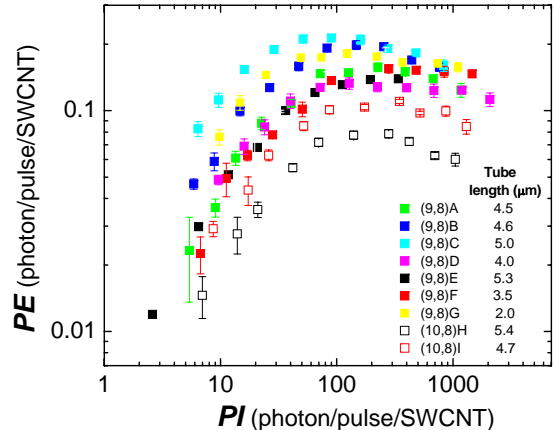


FIG. 2: PL emission for several (9,8) and (10,8) SWCNTs. Error bars indicate standard error of the mean.

By adopting $A = 0.027$ for the absorption coefficient, the number of excitons created per pulse in the SWCNT is derived (using Eq. 1) to be around 3 at the onset of the PL clamping. Considering the length of the nanotubes under study (2 to 5 μm), the annihilation process is much more efficient than expected based on models developed for encapsulated SWCNTs [11, 12, 28]. Application of the diffusion model to our data requires unreasonably high absorption coefficients (orders of magnitude higher than reported here) or dramatically longer linear radiative lifetimes (which would allow much longer diffusion lengths). The analysis of PL as a function of pump fluence determines only the ratio of $\frac{\Gamma}{\Gamma_{NL}}$. To separate linear from nonlinear relaxation rates, we also perform time-resolved PL relaxation experiments using femtosecond excitation correlation spectroscopy (FEC) [29]. A single SWCNT is excited by two equal-intensity pulses separated by variable time delay. Since both pulses are of sufficient intensity to saturate the SWCNT, total PL for both pulses is similar to just one pulse for short time delays. When time delay is increased, relaxation between pulses can occur thus resulting in an increase in the total PL until the point that it is double the initial value (Figure 3 (a), same (9,8)SWCNT as Fig. 1(a)). Note $FEC(t_d)$ is not a direct measurement of exciton relaxation. To interpret it correctly, the FEC signal as a function of time delay, $FEC(t_d)$, is calculated by applying the same stochastic model used above, but for two optical pump pulses separated by delay time (t_d). Modeling shows that for exciton decay with two very different rates (linear and nonlinear), FEC signal is dominated by the slow process (here the mono-exponential linear relaxation) [20]. This explains the FEC signal insensitivity to pump fluence observed in Figure 3 (a). Phase-space filling as previously proposed [29] is not required. In

fact, we are more than two orders of magnitude below the expected Mott density ($> 1 \times 10^6 \text{ cm}^{-1}$) [12]. The whole data set is fitted to a mono-exponential function and yields a time constant of 90 ps.

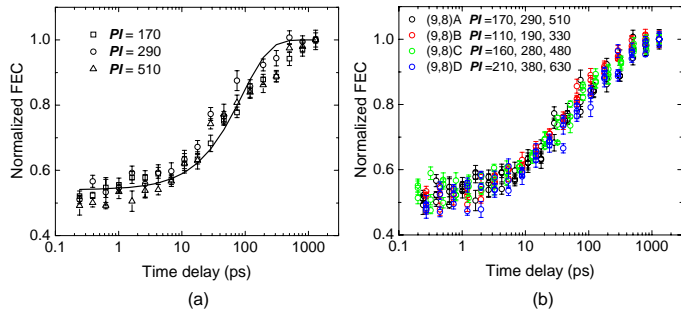


FIG. 3: (a) Normalized SWCNT FEC as a function of time delay between saturating pulses for pump fluences $PI = 170, 290, 510$. Error bars are standard deviations of the mean. Mono-exponential fit (solid curve) yields a time constant of 90 ps. (b) Normalized FEC is very similar for different SWCNTs and different PI .

Similar results are obtained for other SWCNTs (Figure 3 (b)) with time constants ranging over 85 ± 20 ps. This compares to the past results of 10 - 250 ps in encapsulated SWCNTs [8, 9, 14, 30]. Since it appears that air-suspended SWCNTs have similar linear exciton lifetimes, absorption and optical quantum efficiency as high quality encapsulated SWCNTs, we return to their very different nonlinear behavior. Combining the analysis results from PL clamping and FEC, we determine the exciton-exciton annihilation rate in our 2 - 5 μm SWCNT ($\Gamma_{NL} > (0.01 \times 85 \text{ ps})^{-1}$) is the same magnitude or faster than $(0.8 \text{ ps})^{-1}$ that was previously estimated for 380 nm long micelle-encapsulated SWCNTs [28]. This suggests

that with no processing or encapsulation, exciton-exciton interactions in air-suspended SWCNTs are affected by different microscopic processes. Possibilities include very efficient dipole-dipole interaction due to reduced screening, fast coherent exciton transport due to reduced disorder [31], enhanced coupling due to nonlocalized exciton wavefunction overlap, and energy pooling of the excitation to only a few sites on the SWCNT allowing annihilation at very low exciton number [32].

In conclusion, the ability to probe an individual SWCNT suspended in air and identify its parameters (chirality, orientation, length) allow us to determine its intrinsic optical properties and infer its underlying exciton dynamics. Measured PL action cross sections are similar or higher than previously reported consistent with high quality SWCNTs. By investigating the dependence of PL on pump fluence and time resolving SWCNT relaxation, we determine that the stochastic model of exciton relaxation agrees with the experimental results but requires an extremely fast exciton-exciton annihilation rate. An absorption coefficient of $A = 0.02 - 0.06$ indicates interactions between as few as 2 - 6 excitons in a few micron long SWCNT lead to PL clamping. Extremely efficient exciton-exciton annihilation at such low exciton density in the quasi-1D system calls for a new consideration of the nature of excitons optically generated in a SWCNT as well as their interactions.

We acknowledge nanotube sample preparation and characterization by the group including P. Finnie and J. Lefebvre at the Institute for Microstructural Sciences, National Research Council Canada. This work is funded by the Natural Sciences and Engineering Research Council of Canada, the Canadian Foundation for Innovation, and the Ministry of Research and Innovation (Ontario).

-
- [1] J. A. Misewich *et al.* *Science* **300**, 783 (2003).
 [2] M. Freitag *et al.* *Nano Lett.* **3**, 1067 (2003).
 [3] A. Star *et al.* *Nano Lett.* **4**, 1587 (2004).
 [4] M. J. O'Connell *et al.* *Science* **297**, 593 (2002).
 [5] T. Hertel *et al.* *Phys. Status Solidi B* **243**, 3186 (2006).
 [6] M. F. Islam *et al.* *Phys. Rev. Lett.* **93**, 037404 (2004).
 [7] J. Lefebvre *et al.* *Phys. Rev. B* **69**, 075403 (2004).
 [8] A. Hagen *et al.* *Phys. Rev. Lett.* **95**, 197401 (2005).
 [9] A. Högele *et al.* *Phys. Rev. Lett.* **100**, 217401 (2008).
 [10] L. Cognet *et al.* *Science* **316**, 1465 (2007).
 [11] R. M. Russo *et al.* *Phys. Rev. B* **74**, 041405 (2006).
 [12] Y. Murakami and J. Kono, *Phys. Rev. Lett.* **102**, 037401 (2009).
 [13] L. Larry *et al.* *Nat. Phys.* **5**, 54 (2009).
 [14] S. Berciaud *et al.* *Phys. Rev. Lett.* **101**, 077402 (2008).
 [15] J. Lefebvre *et al.* *Nano Lett.* **6**, 1603 (2006).
 [16] D. A. Tsyboulski *et al.* *Nano Lett.* **7**, 3080 (2007).
 [17] K. Kaminska *et al.* *Nanotechnology* **18**, 165707 (2007).
 [18] PE is calculated assuming isotropic SWCNT emission. Reflection from the substrate is considered in axes calibration. Background (recorded with the SWCNT moved away from the excitation spot) has been subtracted.
 [19] Y.-Z. Ma *et al.* *Molecular Physics* **104**, 1179 (2006).
 [20] Y.-F. Xiao *et al.* *Proc. SPIE* **7201**, 720111 (2009).
 [21] Y. Murakami *et al.* *Phys. Rev. Lett.* **94**, 087402 (2005).
 [22] L. J. Carlson *et al.* *Nano Lett.* **7**, 3698 (2007).
 [23] R. J. Ellingson *et al.* *Phys. Rev. B* **71**, 115444 (2005).
 [24] L. Huang and T. D. Krauss, *Phys. Rev. Lett.* **96**, 057407 (2006).
 [25] K. F. Mak *et al.* *Phys. Rev. Lett.* **101**, 196405 (2008).
 [26] A. V. Barzykin and M. Tachiya, *Phys. Rev. B* **72**, 075425 (2005).
 [27] C. Manzoni *et al.* *Phys. Rev. Lett.* **94**, 207401 (2005).
 [28] F. Wang *et al.* *Phys. Rev. B* **70**, 241403 (2004).
 [29] H. Hirori *et al.* *Phys. Rev. Lett.* **97**, 257401 (2006).
 [30] T. Hertel *et al.* *Nano Lett.* **5**, 511 (2005).
 [31] W. Barford and C.D.P. Duffy *Phys. Rev. B* **74**, 075207 (2006).
 [32] P. D. Setz and R. Knochenmuss, *J. Phys. Chem. A* **109**, 4030 (2005).